

1
2 MR. FREDERICK OTU-LARBI (Orcid ID : 0000-0001-6991-1871)

3
4
5 Article type : Primary Research Articles

6
7
8 **Modelling the effect of the 2018 summer heatwave and drought on isoprene emissions in**
9 **a UK woodland**

10 **Running head:** Modelling isoprene emissions during heatwave-drought

11 Frederick Otu-Larbi¹, Conor G. Bolas², Valerio Ferracci³, Zosia Staniaszek², Roderic L.
12 Jones², Yadvinder Malhi⁴, Neil R.P. Harris³, Oliver Wild¹, Kirsti Ashworth¹

13
14 ¹ Lancaster Environment Centre, Lancaster University, LA1 4YQ, UK

15 ² Department of Chemistry, University of Cambridge, Cambridge, CB2 1EW, UK

16 ³ Centre for Environmental and Agricultural Informatics, Cranfield University, Cranfield,
17 MK43 0AL, UK

18 ⁴ Environmental Change Institute, School of Geography and the Environment, University of
19 Oxford, South Parks Road, OX1 3QY, UK

20
21 **Corresponding Authors:**

22 Frederick Otu-Larbi, Email: f.otu-larbi@lancaster.ac.uk, Tel: +44 (0) 7988506983

23 Kirsti Ashworth, Email: k.s.ashworth1@lancaster.ac.uk, Tel: +44 (0) 1524593970

24 Address: Lancaster Environment Centre, Lancaster University, LA1 4YQ

25
26 **Statement of authorship:**

27 All authors designed the experiment and contributed to writing the manuscript. F. Otu-Larbi
28 and K. Ashworth carried out the modelling work and analysed the output data. C. Bolas, V.
29 Ferracci and Z. Staniaszek collected and processed the observational data from Wytham.

30
31 **Conflict of interest statement:** The authors declare no conflict of interest.

32
This article has been accepted for publication and undergone full peer review but has not
been through the copyediting, typesetting, pagination and proofreading process, which may
lead to differences between this version and the [Version of Record](#). Please cite this article as
[doi: 10.1111/GCB.14963](https://doi.org/10.1111/GCB.14963)

This article is protected by copyright. All rights reserved

33 Abstract

34 Projected future climatic extremes such as heatwaves and droughts are expected to have
35 major impacts on emissions and concentrations of biogenic volatile organic compounds
36 (bVOCs) with potential implications for air quality, climate, and human health. While the
37 effects of changing temperature and photosynthetically active radiation (PAR) on the
38 synthesis and emission of isoprene, the most abundant of these bVOCs, are well-known, the
39 role of other environmental factors such as soil moisture stress are not fully understood and
40 are therefore poorly represented in land surface models. As part of the Wytham Isoprene
41 iDirac Oak Tree Measurements (WISDOM) campaign, continuous measurements of isoprene
42 mixing ratio were made throughout the summer of 2018 in Wytham Woods, a mixed
43 deciduous woodland in southern England. During this time, the United Kingdom experienced
44 a prolonged heatwave and drought, and isoprene mixing ratios were observed to increase by
45 more than 400% at Wytham Woods under these conditions. We applied the state-of-the-art
46 FORest Canopy-Atmosphere Transfer (FORCAsT) canopy exchange model to investigate the
47 processes leading to these elevated concentrations. We found that although current isoprene
48 emissions algorithms reproduced observed mixing ratios in the canopy before and after the
49 heatwave, the model underestimated observations by ~40% during the heatwave-drought
50 period implying that models may substantially underestimate the release of isoprene to the
51 atmosphere in future cases of mild or moderate drought. Stress-induced emissions of isoprene
52 based on leaf temperature and soil water content were incorporated into current emissions
53 algorithms leading to significant improvements in model output. A combination of soil water
54 content, leaf temperature and rewetting emission bursts provided the best model-
55 measurement fit with a 50% improvement compared to the baseline model. Our results
56 highlight the need for more long-term ecosystem-scale observations to enable improved
57 model representation of atmosphere-biosphere interactions in a changing global climate.

58 **Key phrases:** Isoprene emissions, Isoprene mixing ratios, Heatwave-drought, Soil Water
59 Content, Rewetting, Canopy exchange modelling, Climate change

60

61 Introduction

62 The biogenic volatile organic compound (bVOC) isoprene (C_5H_8), has important
63 impacts on atmospheric composition and chemistry due to its relative abundance and high
64 reactivity (e.g. Fuentes et al., 2000; Laothawornkitkul, Taylor, Paul, & Hewitt, 2008).
65 Chemical reactions involving isoprene lead to the production of secondary pollutants, e.g.
66 ozone (O_3) and secondary organic aerosol (SOA), which are also short-lived climate forcers.

67 Isoprene also indirectly affects climate by reducing the oxidative capacity of the atmosphere,
68 hence enhancing the atmospheric lifetime of climate active gases such as methane (CH₄; see
69 e.g. Pike & Young, 2009). Increased isoprene emissions could potentially lead to up to a 50%
70 change in surface ozone concentrations (Pike & Young, 2009) but the sign of change depends
71 on geographical location and atmospheric composition, in particular on the concentrations of
72 the oxides of nitrogen (NO_x=NO+NO₂). The large quantities of isoprene emitted into the
73 atmosphere make it a major source of SOA although aerosol yield from isoprene depends on
74 a number of factors including levels of organic aerosol loading and NO_x concentrations
75 (Carlton, Wiedinmyer, & Kroll, 2009). SOA has an indirect impact on climate through
76 changing cloud optical properties (Carslaw et al., 2010; Unger, 2014). Isoprene and other
77 bVOCs have been estimated to have a net negative radiative forcing which offsets the
78 positive radiative forcing of anthropogenic volatile organic compounds (Unger, 2014).
79 Isoprene could therefore play an important role in future climates through its regulation of
80 atmospheric chemistry and formation of secondary pollutants, although its overall climate
81 impact is minor compared to greenhouse gases such as CO₂, and remains uncertain (Arneth et
82 al., 2010).

83 More than 90% of global isoprene is emitted by terrestrial vegetation (Guenther et al.,
84 2006) at a rate primarily dependent on vegetation type (with forests contributing ~80% of
85 global annual emissions) but also on environmental conditions such as temperature, solar
86 radiation, atmospheric CO₂ concentration and soil moisture (Guenther et al., 2006 and
87 references therein; Laothawornkitkul et al., 2008). Several hypotheses have been proposed to
88 explain why some plants synthesise and emit isoprene, the best supported being that it
89 prevents cellular damage caused by heat and oxidative stress (e.g. Sharkey, 2000; Vickers,
90 Gershenson, Lerdau, & Loreto, 2009). Hence emissions increase under high temperature and
91 insolation.

92 During periods of water stress, however, physiological processes such as stomatal
93 conductance, photosynthesis rate and respiration are reduced, resulting in a decrease in plant
94 productivity (Keenan, Sabate, & Gracia, 2010). Isoprene emissions are closely coupled with
95 photosynthesis and so reductions in plant photosynthetic capacity as a result of water stress
96 would be expected to lead to a decrease in isoprene emissions by reducing the supply of
97 carbon available for its synthesis. Indeed, studies have observed decreases in isoprene
98 emission rates of between 40-60% under severe drought conditions (e.g. Brüggemann &
99 Schnitzler, 2002; Lerdau et al; 1997; Pegoraro et al., 2004a; Brilli et al., 2007).

100 However an increase in emissions under drought has also been reported (Brilli et al.,
101 2007; Loreto & Schnitzler, 2010; Rennenberg et al., 2006; Sharkey & Loreto, 1993)
102 suggesting that water stress can decouple isoprene emission from photosynthesis, possibly
103 because isoprene emissions are unaffected by decreasing stomatal conductance (Centritto,
104 Brilli, Fodale, & Loreto, 2011; Pegoraro et al., 2004; Tingey, Evans, & Gumpertz, 1981).
105 Experiments using ^{13}C labelling have shown that isoprene can be produced from older pools
106 of stored carbon when photosynthetic gas exchange is reduced by drought (e.g. Brilli et al.,
107 2007).

108 The net impact of soil water stress on isoprene emissions remains uncertain due to these
109 competing effects. It is likely that the apparently contradictory responses observed in
110 laboratory experiments are due to differences in the severity of the applied drought and the
111 tolerance of different plant species to water stress, with severe drought, in which the soil
112 water content (SWC) falls below the permanent wilting point, leading to a decline in isoprene
113 emissions and mild to moderate drought having either no impact or leading to an increase.
114 Niinemets (2010) developed a conceptual model in which the initial increase in leaf
115 temperature that occurs as stomata close in response to a decline in soil moisture stimulates
116 isoprene synthesis and emissions, leading to the observed decoupling of emissions from gas
117 exchange rates. Evidence for this model was later provided by Potosnak et al. (2014) who
118 observed this behaviour at the onset of a prolonged drought in the Ozarks, an oak-dominated
119 mid-latitude forest.

120 An additional complexity is the response of isoprene emission rates to rewetting.
121 Sharkey & Loreto (1993) and Peñuelas, Filella, Seco, & Llusia (2009) observed a substantial
122 increase in isoprene emissions from seedlings after rewetting but this effect has not been
123 observed in all experiments. Pegoraro et al (2004) reported a lag of about a week between
124 declining soil moisture and changes in isoprene emission rates most likely the result of plants
125 having to adjust to the restoration of the photosynthetic carbon source for isoprene synthesis
126 and emission.

127 The effect of temperature and solar radiation on isoprene emissions are relatively well
128 understood and emissions estimates from land surface models have been shown to capture
129 observed diurnal variations in fluxes and concentrations reasonably effectively across a range
130 of ecosystems (e.g. Guenther et al., 2012; Zimmer et al., 2000). Unlike temperature and solar
131 radiation, there is no direct impact of soil water deficit and soil rewetting on isoprene
132 emissions and these are therefore not well represented in coupled land surface-atmosphere
133 models although numerous studies have shown their importance to emission rates and

134 atmospheric composition (e.g. Emmerson, Palmer, Thatcher, Haverd, & Guenther, 2019;
135 Guenther et al., 2006; Jiang et al., 2018; Sindelarova et al., 2014).

136 Rising levels of CO₂ and future changes in climate, such as increasing temperature and
137 altered patterns of precipitation, can thus be expected to change isoprene emissions from the
138 current estimated 450–600 Tg C y⁻¹ (Arneth, Monson, Schurgers, Niinemets, & Palmer,
139 2008; Guenther et al. 2006; 2012). Heald et al. (2009) projected increases of as much as ~190
140 Tg C y⁻¹ in global isoprene emissions due to a temperature increase of 2.3°C by 2100, but
141 also showed that a decrease in isoprene emissions due to increasing CO₂ concentrations could
142 off-set this temperature effect almost entirely.

143 Most studies to understand the effect of combined heatwaves and drought on isoprene
144 emissions have been laboratory-based experiments which permit close control of
145 environmental factors such as temperature, photosynthetic active radiation (PAR) and soil
146 moisture but make use of saplings (e.g. Brillì et al., 2007), seedlings or young plants (e.g.
147 Pegoraro et al., 2005) and are thus not representative of real-world forest environments.
148 There are limited observations of isoprene emissions during drought in natural ecosystems
149 (e.g. Emmerson et al., 2019; Potosnak et al., 2014; Seco et al., 2015) which are necessary to
150 enable the development of robust parameterisations in emissions models.

151 In the summer of 2018, the United Kingdom (UK), in common with most of northern
152 and central Europe, experienced a prolonged drought and heatwave event. The UK Met
153 Office officially declared heatwave conditions starting on June 22nd which persisted to
154 August 8th in southern England. Records from the UK Met Office shows that the 2018
155 summer mean temperature over the UK as a whole was ~2.0°C above the 1961-1990 average,
156 making the summer of 2018 the joint warmest on record (“Regional Values”, 2019). The
157 mean temperature over southern England was 17.7°C, ~2.4°C warmer than the 1961-1990
158 average.

159 Under future climate scenarios, droughts and heatwaves that are currently thought of as
160 anomalous (such as the one that occurred in 2018) are expected to increase in frequency
161 (IPCC, 2013; Thornton, Ericksen, Herrero, & Challinor, 2014) with the UK Met Office
162 predicting that the UK may experience such conditions every other year by 2050 (e.g “UK
163 Extreme Events – Heatwaves”, 2019). Given the role of isoprene and other BVOCs in the
164 formation of short-lived climate forcers and secondary organic aerosols (SOA), the potential
165 impacts of these changes in climate on isoprene emission rates and therefore on atmospheric
166 composition, air quality and climate (Sanderson, Jones, Collins, Johnson, & Derwent, 2003;
167 Pacifico, Harrison, Jones, & Sitch, 2009) must be better understood.

168 The combined heatwave and drought (heatwave-drought) and rewetting episodes
169 that occurred during the Wytham Isoprene iDirac Oak Tree Measurements (WIsDOM)
170 campaign in Wytham Woods in 2018, offered a unique opportunity to quantify the potential
171 effect of future climate change on isoprene emissions in a natural environment. This study
172 uses a state-of-the-art canopy model to explore the observed effects of heat and drought
173 stress, and soil rewetting on isoprene emissions and mixing ratios in a temperate mixed
174 deciduous woodland.

175 **Methods**

176 **Site Description**

177 The WIsDOM campaign took place at Wytham Woods (51°46'23.3"N 1°20'19.0"W, 160
178 m.a.s.l), located ~5km NW of the centre of Oxford in SW England, between May-October
179 2018. The forest has been owned and maintained by the University of Oxford as a site of
180 special scientific interest since 1942 and has been part of the UK Environmental Change
181 Network (ECN) since 1992. The forested area is made up of patches of ancient semi-natural
182 woodland, secondary woodland, and modern plantations and is dominated by European Ash
183 (*Fraxinus excelsior* - 26%), Sycamore (*Acer pseudoplatanus* - 18%), European Beech
184 (*Fagus sylvatica* - 11%) and English Oak (*Quercus robur* - 7%; Kirby et al., 2014). The
185 remainder of the forest comprises other broadleaf trees and shrubs. *Q. robur* (~95%) and *A.*
186 *pseudoplatanus* (~5%) are the main contributors to the isoprene budget at Wytham Woods
187 (Bolas, 2020). The forest has largely been undisturbed over the last 40-100 years (Morecroft,
188 Stokes, Taylor, & Morison, 2008; Thomas et al., 2011) and as a consequence the age range of
189 mature trees in Wytham Woods is large - from 40 to >150 years. The climate in Oxfordshire
190 can be classified as warm temperate with rainfall occurring all year round. The 1981-2010
191 average summer temperature ranges between 18-20 °C and average rainfall is ~600-700 mm
192 per year.

193 **Measurement Campaign**

194 Continuous measurements of isoprene mixing ratios were made approximately every 20
195 minutes at four heights in the forest canopy between June-October 2018 during the WIsDOM
196 campaign. Inlets to two dual-channel iDiracs (see Bolas et al., 2019 for a full description of
197 the instrument design and deployment) were located at 15.55m (top of canopy), 13.17 m
198 (mid-canopy), 7.26 m (trunk height) and 0.53 m (near surface) alongside a mature *Q. robur*
199 of ~16 m height. Measurements at the trunk and near surface levels did not start until July.
200 The iDirac has a detection limit of ~38 ppt with an instrument precision of ±11% (Bolas et
201 al., 2019).

Hourly measurements of temperature, PAR, relative humidity, soil moisture at a depth of 20cm, wind speed and direction, and atmospheric pressure were obtained from the Upper Seeds automatic weather station (AWS) located in a small clearing ~480 m from the site of the isoprene observations. We used 30-minute averages of the measurements made between 1st June to 30th September in our model analysis. This covers the full extent of peak growth with roughly equal periods before, during and after the heatwave-drought. For full details of the WISDOM campaign, readers are referred to Ferracci et al. (2020).

Model Description

We applied the FORest Canopy-Atmosphere Transfer (FORCAsT) 1-D model of biosphere-atmosphere exchange to simulate the processes of biogenic emissions, chemical production and loss, vertical mixing, advection and deposition within and above the canopy at Wytham Woods. A detailed description of the FORCAsT model can be found in Ashworth et al. (2015), so here we focus only on those elements of the model configuration relevant to this study. We subdivided the 40 model levels into 10 between the ground surface and trunk height, and a further 10 within the crown space to ensure that observation heights aligned as closely as possible with the mid-point of a model level.

Vertical transport in FORCAsT is based on a modified k-theory of vertical turbulent diffusion (Blackadar, 1962; Raupach, 1989). In-canopy and above canopy mixing are simulated following Baldocchi (1988) and Gao et al. (1993) respectively. The simulated exchange of heat and trace gases are further improved by constraining the friction velocity (u^*) and the standard deviation of the vertical wind component (σ_w) following Bryan et al. (2012). As u^* and σ_w were not measured at Wytham we estimated each from the horizontal wind speed (u) following Makar et al., (2017), Eqn. 1, and Shuttleworth and Wallace (1985), Eqn. 2, respectively:

$$u^* = \frac{u \times K}{\ln\left(\frac{h_c}{z_o}\right)} \quad (1)$$

$$\sigma_w\left(\frac{z}{h_c}\right) = \begin{cases} 1.25u^* & \text{for } \frac{z}{h_c} > 1.0 \\ u^* \left[0.75 + 0.5 \times \cos\left(\pi\left(1 - \frac{z}{h_c}\right)\right)\right] & \text{for } \frac{z}{h_c} < 1.0 \end{cases} \quad (2)$$

where h_c is height of top of canopy (18m), Z_o is roughness length (assumed $0.1 \cdot h_c$), u is mean horizontal windspeed at height z and K is von Karman's constant (0.4).

In FORCAsT, isoprene is produced through emissions from foliage in the crown space and lost through oxidation reactions initiated by the OH and NO₃ radicals and O₃, and

232 through deposition to the soil (following Stroud et al., 2005). The concentration of isoprene at
 233 each level in the canopy depends on these production and loss processes as well as fluxes into
 234 and out of that layer. Previous studies (e.g. Bryan et al., 2012; Guenther et al., 2006 and
 235 references therein) have shown that for moderate height canopies such as that at Wytham
 236 Woods, canopy residence times are sufficiently short that little isoprene is lost through
 237 oxidation within the canopy. Hence, concentrations are primarily dependent on emission rates
 238 when considered over periods greater than turbulent timescales (≤ 1 s to minutes). FORCAsT
 239 employs a half-hourly timestep. Our simulations therefore focused on the emissions of
 240 isoprene, which are calculated in FORCAsT by summing the contributions from 10 leaf angle
 241 classes in each crown-space model level, following the algorithms of Guenther et al. (1995):

$$242 \quad ER = LAI \cdot \epsilon \cdot \gamma_{iso} \quad (3)$$

243 where ER is the total emission rate ($\text{mg m}^{-2} \text{h}^{-1}$), LAI ($\text{m}^2 \text{m}^{-2}$) is the leaf area index and ϵ is a
 244 site- and species-specific emission factor ($1.20 \text{ mg m}^{-2} \text{h}^{-1}$ for *Q. robur*; Visakorpi et al.,
 245 2018) which represents the emission rate of isoprene into the canopy at standard conditions of
 246 $30 \text{ }^\circ\text{C}$ and $1000 \text{ } \mu\text{mol m}^{-2} \text{s}^{-1}$. LAI was taken as the maximum reported for the site ($3.6 \text{ m}^2 \text{m}^{-2}$;
 247 Herbst et al., 2008) throughout this study which coincides with the period of peak growth.
 248 γ_{iso} is a dimensionless emission activity factor that accounts for changes in emission rates due
 249 to deviations from these standard conditions, with:

$$250 \quad \gamma_{iso} = C_L C_T \quad (4)$$

251 where C_L and C_T are the light and temperature dependence of isoprene emission rates
 252 respectively and are given by:

$$253 \quad C_L = \frac{\alpha C_{LI} PAR}{\sqrt{1 + \alpha^2 PAR^2}} \quad (5)$$

254 where α ($= 0.0027$) and C_{LI} ($= 1.066$) are empirical coefficients from Guenther et al. (1995).

$$255 \quad C_T = \frac{\exp\left(\frac{C_{T1}(T - T_s)}{RT_s T}\right)}{1 + \exp\left(\frac{C_{T2}(T - T_m)}{RT_s T}\right)} \quad (6)$$

256 where T is leaf temperature (K), T_s is the temperature at standard conditions (i.e. 303 K), R is
 257 the ideal gas constant ($= 8.314 \text{ J K}^{-1} \text{ mol}^{-1}$), C_{T1} ($= 95,000 \text{ J mol}^{-1}$), C_{T2} ($= 230,000 \text{ J mol}^{-1}$)
 258 and T_m ($= 314 \text{ K}$) are empirical coefficients determined by Guenther et al. (1995). Leaf
 259 temperature is calculated from measured air temperature in FORCAsT using a canopy energy
 260 balance.

261 Equations (3) to (6) describe the default model set-up (hereafter referred to as BASE).
 262 We conducted a series of experiments introducing stress-induced emissions, achieved by

263 further modifying the activity factor to account for extreme temperature and drought
264 conditions. In these experiments, described below, γ_{iso} was calculated as:

$$265 \quad \gamma_{iso} = C_L C_T \gamma_X \quad (7)$$

266 where γ_X is an additional environmental activity factor and x denotes the environmental
267 condition affecting isoprene emission rates in each experiment- explained in detail below.

268 **Model experiments**

269 **BASE:** FORCAsT was configured using site-specific canopy parameters and isoprene
270 emission factors and driven with meteorology measured at Wytham Woods during the
271 WIsDOM campaign. Isoprene emission rates for each model level were calculated within the
272 model using Eqns. 3-6. Comparison of modelled isoprene mixing ratios against observations
273 from the iDirac instruments at four heights within the canopy showed good agreement in both
274 diurnal profile and magnitude before and after the heatwave-drought. However, during the
275 heatwave-drought period the model substantially underestimated isoprene mixing ratios. The
276 results from this simulation are described in more detail later.

277 We therefore performed three subsequent experiments, introducing γ_X , to explore the
278 possible environmental factors driving the sharp increase in observed isoprene concentrations
279 that the model was unable to account for using the standard emissions algorithms. In all three
280 experiments, model configuration and driving meteorology remained unchanged from BASE;
281 the only difference was the change to the isoprene activity factor described below.

282 **BASE+LFT:** During periods of drought stress there is an increase in leaf temperature
283 due to a reduction in transpiration rate as the plants attempt to conserve water (Zandalinas,
284 Mittler, Balfagón, Arbona, & Gómez-Cadenas, 2018). Niinemets (2010) and Potosnak et al.
285 (2014) hypothesised that this increase in leaf temperature is the cause of observed increases
286 in isoprene emissions during mild-to-moderate drought stress. Here we test whether increases
287 in leaf temperature explain the observed changes in isoprene mixing ratios observed during
288 WIsDOM by modifying γ_X against leaf temperature (hereafter referred to as LFT) with γ_{LFT}
289 defined as:

$$290 \quad \gamma_{LFT} = \begin{cases} 1 & T < T_{95} \\ \frac{T - T_s}{T_{95} - T_s} & T \geq T_{95} \end{cases} \quad (8)$$

291 where T (K) is the leaf temperature, T_s (297K) represents standard conditions for leaf
292 temperature (Guenther et al., 2006) and T_{95} is the 95th percentile of the seasonal leaf
293 temperature which represents the threshold temperature above which we assume heat-induced
294 emissions occur.

295 **BASE+SWT:** Under heatwave-drought conditions it would be expected that reduced
296 SWC and unusually high temperatures affect emissions rates simultaneously. This
297 experiment therefore combines the effect of soil water deficit and leaf temperature on
298 isoprene emissions into a single environmental activity factor, γ_{SWT} calculated as follows:

$$299 \gamma_{SWT} = \begin{cases} 1 & \text{for } \theta > \theta_c \\ \left[\frac{(\theta - \theta_w)}{\theta_c - \theta_w} \right]^q \times [\gamma_{LFT}] & \text{for } \theta_w < \theta \leq \theta_c \end{cases} \quad (9)$$

300 where θ ($\text{m}^3 \text{m}^{-3}$) is the volumetric soil moisture, θ_w is the wilting point ($0.15 \text{ m}^3 \text{m}^{-3}$
301 following Jiang et al., 2018), θ_c ($0.22 \text{ m}^3 \text{m}^{-3}$) is a critical soil moisture content above which
302 we observe no effect of water stress on isoprene emissions and q is a site-specific empirical
303 factor describing the non-linearity of the effects of soil water stress on tree physiological
304 processes. A range q values have been tested for different plant functional types (eg. see Egea
305 et al., 2011). Here a value of 0.40 provided the best fit to observations. γ_{LFT} is defined in
306 Eqn 8.

307 **BASE+RWT:** This experiment investigates whether the burst of isoprene emissions
308 observed following re-wetting after drought in laboratory studies is seen at the ecosystem
309 scale. The environmental activity factor, γ_{RWT} , is a modification of Eqn 9 such that during
310 periods defined as rewetting (days within the heatwave-drought period for which soil water
311 content exceeds that of the previous 10 days), γ_{RWT} is given by:

$$312 \gamma_{RWT} = \gamma_{SWT} \times 1.30 \quad (10)$$

313 i.e. a 30% increase in isoprene emissions following soil rewetting.

314 **Results**

315 Here we present a comparison of continuous measurements of isoprene mixing ratios at
316 all four iDirac inlet levels against the output from the nearest model level. For the top and
317 middle of the canopy, we use half-hourly averages of both modelled and observed data
318 covering the period June 1st to September 30th for this comparison; measurements are only
319 available for the trunk and near surface levels between July 6th and September 30th. Statistical
320 values reported in this section were restricted to isoprene mixing ratios between 0600 LT to
321 1900 LT coinciding with daylight hours when isoprene emissions occur, in keeping with
322 previous studies (e.g. Potosnak et al., 2014; Seco et al., 2015). The data is presented in full as
323 time series, and then summarised to show goodness of fit using scatter plots and a Taylor
324 diagram (Taylor, 2001). The Taylor diagram provides a way to demonstrate the simultaneous
325 variation of three model performance statistics: correlation coefficient (r^2), normalised
326 standard deviation (SD), and centred root-mean-square error (RMSE). Output from an ideal

327 model would show the same r^2 , SD and RMSE as the observations. Therefore, the closer a
328 model's summary statistics are to that of the observations on the Taylor diagram, the better its
329 performance. Results are first presented for the BASE simulation (i.e. the default model set-
330 up) and then for each experiment. Model performance statistics for the top of the canopy is
331 presented here while those for the other levels can be found in the Supplementary
332 Information (SI). The grey shaded region on all figures indicates the heatwave-drought period
333 as defined by the UK Met Office for southern England and the dashed white line the start of
334 re-wetting.

335

336 **Meteorological conditions**

337 Figures 1a-c show PAR, temperature, volumetric SWC, and precipitation measured at
338 the ECN station in Wytham Woods for the study period. Following a wet April in which
339 rainfall was ~120% of the 1981-2010 mean ("Monthly, seasonal and annual summaries
340 2018"; 2019), SWC declined steadily from near field capacity (at $0.46 \text{ m}^3 \text{ m}^{-3}$) at the start of
341 June to $0.16 \text{ m}^3 \text{ m}^{-3}$ (just above the wilting point of $0.15 \text{ m}^3 \text{ m}^{-3}$ for this site) at the peak of the
342 heatwave-drought in July. A few low-intensity rainfall events (total precipitation $<0.2 \text{ mm}$)
343 with negligible effect on SWC were recorded prior to the heatwave-drought. Rainfall during
344 the heatwave-drought, on July 20th (3 mm) and July 27th (11.1 mm), led to increases in soil
345 moisture and the "rewetting period" extended from 20th July to 8th August as a result. The
346 Standardized Precipitation Index (SPI; McKee, Doesken, & Kleist, 1993), used to
347 characterize the severity of meteorological droughts, indicates Wytham Woods experienced a
348 moderate drought in July (<https://eip.ceh.ac.uk/apps/droughts/>), consistent with in-situ SWC
349 measurements. After 8th August (the official end of the heatwave period), rainfall frequency
350 and intensity increased with a corresponding increase in soil moisture.

351 The average temperature recorded at Wytham Woods was 17.5°C for the entire
352 measurement period (1st June-30th Sept), but 19.6°C during the heatwave (22nd June-8th Aug).
353 The diurnal temperature ranged from an average of 11.8°C at night to 21.3°C during the day
354 for the whole season but increased sharply during the heatwave, with mean night-time and
355 daytime temperatures of 13.5°C and 25.2°C respectively. For the same June to September
356 period, climatological (1993-2015) temperature averaged 15.8°C with a diurnal range of
357 10.2°C - 18.9°C . Compared to the long-term average, the 2018 summer at Wytham Woods was
358 1.7°C warmer mainly due to a 3.0°C increase in temperature during the heatwave-drought.
359 The maximum temperature recorded at Wytham Woods during the 2018 heatwave-drought
360 (30.6°C) was however lower than the climatological maximum (32.2°C). Average PAR

361 increased from 781 W m^{-2} before the heatwave-drought to 1277 W m^{-2} during it, reflecting
362 longer and more intense periods of sunshine associated with the underlying high pressure
363 conditions of the heatwave period.

364 [FIGURE 1 GOES APPROXIMATELY HERE]

365 **BASE model simulation**

366 As isoprene emission rates are predominantly determined by light and temperature,
367 BASE reliably reproduces the diurnal cycle of isoprene concentrations at each of the inlet
368 levels (Figure 2 (a-d)). Average modelled mixing ratios outside of the heatwave-drought are
369 in good agreement with those observed (0.44 ppb vs. 0.37 ppb at the top of the canopy, 0.24
370 ppb vs. 0.18 ppb at mid-canopy level, 0.17 ppb vs. 0.15 ppb at trunk level and 0.09 ppb vs.
371 0.11 ppb near the surface), with no apparent systematic bias, suggesting that the emission
372 factor, ϵ , is appropriate for the site. However, FORCAsT underestimates concentrations at all
373 levels during the heatwave-drought by an average of 40% leading to a total underestimation
374 of ~25% over the entire season. During the heatwave-drought, the average isoprene mixing
375 ratio measured at the top of the canopy was 1.97ppb (i.e. > 4 times that outside the heatwave
376 period) but only 1.12 ppb in BASE. Similar results were obtained at the other levels for
377 model vs observations (1.01 ppb vs 0.60 ppb at mid-canopy level, 0.84 ppb vs 0.49 ppb at
378 trunk level and 0.58 ppb vs 0.15 ppb near the surface). Following the two rewetting episodes
379 in July, average observed isoprene mixing ratios increased to 2.05 ppb, while modelled
380 isoprene was nearly a factor of 2 lower at 1.12 ppb for that period. There was a 48%, 44%
381 and 70% underestimation in the model at the mid-canopy, trunk and near surface levels
382 respectively, following the rewetting events. These systematic discrepancies show that the
383 emission burst observed following rewetting is unaccounted for in current emissions
384 algorithms.

385 [FIGURE 2 GOES APPROXIMATELY HERE]

386 The time series of the difference between modelled and observed isoprene mixing ratios
387 at the top of the canopy for BASE (Figure 3a) highlights the relatively poor skill of the
388 standard emissions algorithms throughout the 7-week heatwave-drought (shaded region). The
389 average diurnal profiles of isoprene mixing ratios before, during and after the heatwave-
390 drought presented in Figure 3(b) further confirm the good performance of BASE before and
391 after the heatwave and the substantial underestimation during the heatwave. Figures 3(c-d)
392 explore the relationship between these differences and the possible environmental drivers:
393 SWC and temperature. Figure 3(c) points to a soil moisture threshold with isoprene mixing
394 ratios (and therefore emissions) independent of SWC above $\sim 0.22 \text{ m}^3 \text{ m}^{-3}$ but increasing

395 rapidly as SWC drops further. This is in keeping with the concept of a critical SWC used in
396 modelling both photosynthesis and isoprene emissions in previous work (e.g. Emmerson et
397 al., 2019; Guenther et al., 2006; Keenan et al., 2010) although we see an increase rather than
398 decrease as SWC declines below this threshold, similar to that reported under moderate
399 drought stress by Potosnak et al. (2014). Figure 3(d) suggests a similar but less pronounced
400 response to high temperatures ($>20^{\circ}\text{C}$). We found no significant relationship between PAR
401 and the difference between modelled and measured isoprene mixing ratios and conclude that
402 high temperature and low SWC are the key drivers of the apparent stress-induced
403 enhancement in isoprene emissions.

404 [FIGURE 3 GOES APPROXIMATELY HERE]

405

406

407 **Results of Modelling Experiments**

408 Figures 2 and 3 show clearly that BASE underestimated isoprene concentrations during
409 the heatwave-drought and at other times when isoprene levels in the canopy were high. In this
410 section we present the results of our model experiments exploring the addition of stress-
411 induced emissions and compare them to the performance of BASE over the entire season. As
412 for BASE, model performance statistics are similar for all levels for each experiment. We
413 therefore present only statistics for top of the canopy here; statistics for the other levels are
414 given in Table S1 in the SI.

415 **BASE+LFT:** Modifying the isoprene activity factor when leaf temperature exceeds the
416 95th percentile (γ_{LFT}) reduces the net underestimation during the heatwave-drought but, as
417 shown in Figure 4(a) and E, FORCAST still substantially underestimates observed mixing
418 ratios throughout this period. The average modelled isoprene mixing ratio is 1.26 ppb during
419 the heatwave-drought (~35% lower than observed) and 0.76 ppb (25% too low) over the
420 entire season. This tendency towards underestimation can be seen clearly in Figure 5(b) and
421 (f) (most of the points lie below the 1:1 line) as can the improvement over the performance of
422 BASE (shown in Figure 5(a) and e). Figure 6 further confirms that the use of a temperature-
423 induced enhancement (γ_{LFT}) in isoprene emissions improves the overall fit to measurements.
424 The RMSE of modelled mixing ratio is reduced (from 0.60 in BASE to 0.57 in BASE+LFT),
425 reflecting a slightly improved accuracy during the heatwave-drought. The normalised
426 standard deviation

427 (0.61 in BASE vs 0.66 in BASE+LFT) indicates that the model is also better able to
428 reproduce the variability seen in the observed concentrations although still tending to

429 underestimate. It should be noted that the correlation between modelled and observed
430 isoprene is very good (>0.9) for all simulations as the strong dependency of isoprene
431 emissions on temperature and PAR is well-captured by the standard emissions algorithms
432 (Eqns. 3-6) included in BASE. Figure 6 shows that although BASE+LFT improves model
433 reproduction of isoprene mixing ratios, it is still unable to account for the high concentrations
434 during the heatwave-drought and suggests that other factors are responsible for the increase
435 in isoprene concentration during this period.

436 **BASE+SWT:** This experiment accounted for the simultaneous effect of heat and water
437 stress. As shown in Figure 4(b) and (e), there is a clear improvement in the model's
438 estimation of isoprene mixing ratios during the heatwave-drought period compared to both
439 BASE and BASE+LFT and this is further confirmed by Figure 5(c) and (g), in which most
440 points lie along or close to the 1:1 line. Fig 5(c) and (g) also show that BASE+SWT
441 consistently underestimates when observed mixing ratios are high (>5 ppb and >3 ppb at the
442 top and middle of the canopy respectively). The mean modelled isoprene mixing ratio at the
443 top of the canopy is 1.87ppb, just $\sim 5\%$ lower than the observed value of 1.97ppb. There are
444 no periods of consistent model bias, rather FORCAST underestimates isoprene concentrations
445 periodically through the heatwave period, resulting in the standard deviation <1.0 in Figure 6.
446 Referring to Figure 1(b), it can be seen that these periods of underestimation correspond to
447 rewetting periods following rainfall events. The average modelled mixing ratio during the
448 rewetting period was 1.73ppb compared to the observed value of 2.05ppb. This constitutes
449 $\sim 15\%$ underestimation compared to observed values but $\sim 35\%$ increase (improvement) over
450 the 1.12ppb and 1.11ppb estimated in BASE and BASE+LFT respectively.

451 **BASE+RWT:** The final experiment included an additional 30% enhancement of the
452 environmental activity factor following soil rewetting (γ_{RWT}) and, as shown in Figure 4(c)
453 and F, further improves the model performance during the heatwave-drought. Mean isoprene
454 mixing ratios during this period increase from 1.87 ppb in BASE+SWT to 1.98 ppb in
455 BASE+RWT, equal to the average of observed values. Figure 5(d) and (h) indicates no
456 systematic model bias and the use of a rewetting-enhanced soil moisture activity factor
457 enables the model to capture the higher observed concentrations following rewetting episodes
458 which all previous simulations failed to reproduce. The average isoprene mixing ratio during
459 these re-wetting periods is 1.98 ppb compared to 2.05 ppb in the observations, i.e. an
460 underestimation of only $\sim 3\%$. The overall model performance statistics are depicted in Figure
461 6. While there is no significant difference between the overall correlation or RMSE values in

462 BASE+SWT and BASE+RWT, there is a clear improvement in the model's ability to match
463 the variability shown by the observations with a normalised standard deviation of 0.97 in
464 BASE+RWT compared to 0.89 in BASE+SWT. Compared to BASE, there is ~80% and
465 ~50% improvement in SD (0.97 in BASE+RWT vs 0.61 in BASE) and RMSE (0.41 in
466 BASE+RWT vs 0.60 in BASE) respectively.

467 [FIGURE 4 GOES APPROXIMATELY HERE]

468 [FIGURE 5 GOES APPROXIMATELY HERE]

469 [FIGURE 6 GOES APPROXIMATELY HERE]

470 [FIGURE 7 GOES APPROXIMATELY HERE]

471 **Time series of Results**

472 Figure 7 shows isoprene mixing ratios for the period July 22nd-27th 2018, selected as it
473 falls within the heatwave-drought and includes the first of the rainfall events. These plots
474 provide further evidence that all model configurations reproduce the observed diurnal
475 patterns of isoprene concentrations at Wytham Woods at the top 3 levels, as expected given
476 the strong dependency of isoprene emissions on temperature and PAR but confirm the earlier
477 results from Figure 2 and Figure 4 that BASE and BASE+LFT models systematically and
478 substantially underestimate isoprene mixing ratios during this period. All three experiments
479 improve model estimations of isoprene concentrations over BASE especially during the
480 middle of the day when observed concentrations peak. Figure 7(a-d) show clearly the effect
481 of adding a rewetting-induced enhancement in isoprene emissions (Eqn 10). For 22nd July,
482 when the rewetting effect is not active, the BASE+SWT and BASE+RWT lines overlap but
483 they diverge between 23rd-27th July following rewetting. Figure 7(h) shows that all the
484 simulations underestimate observed concentrations near the surface in the early part of the
485 morning (before mid-day), which we ascribe to more light reaching the lower levels in the
486 canopy than is currently accounted for in the model. Figure 7 confirms that BASE+RWT
487 provides the overall best fit when compared to the observations at all levels.

488

489 **Discussion**

490 Wytham Woods experienced a heatwave and moderate drought (heatwave-drought)
491 during a 7-week period in the summer of 2018 during which time the soil moisture at the site
492 decreased from 0.46 m³ m⁻³ (just below field capacity) to 0.16 m³ m⁻³ (just above wilting
493 point). Continuous measurements of isoprene mixing ratios were made at the site during the
494 Wytham Isoprene iDirac Oak Tree Measurements (WIsDOM) campaign which was

495 conducted in May-October 2018. The aims of our study were to determine how well a 1-D
496 canopy exchange model (FORCAsT) could capture the observed changes in isoprene
497 concentrations during the heatwave-drought and to use the model to explore the
498 environmental factors driving these changes. Modelled isoprene mixing ratios did increase
499 substantially during the heatwave-drought in response to large increases in foliage emissions,
500 driven by high temperature and PAR, but not to the extent observed. We conclude that the
501 algorithms currently used in emissions models are unable to account for the actual increase in
502 emission rate under such conditions. We hypothesise that the increase in emission rates
503 during the heatwave-drought was most likely a mechanism to cope with abiotic stress as
504 previously suggested by Holopainen (2004); Loreto & Velikova (2001); Peñuelas & Llusà
505 (2002); Sharkey (1996), and in particular due to low soil moisture.

506 Many previous studies of the effect of soil water deficit on isoprene emissions have
507 shown a decrease in emission rates with increasing severity of drought (e.g. Pegoraro et al.,
508 2005; Seco et al., 2015) leading to the development of algorithms that decrease the isoprene
509 activity factor (γ_{iso}) in response to decreasing SWC (Guenther et al., 2006). This approach has
510 been used in emission models (e.g. Emmerson et al 2019; Guenther et al., 2006; Jiang et al.,
511 2018) with good results for severely drought-impacted sites. However, other studies have
512 reported that isoprene emissions are enhanced during periods of mild or moderate drought
513 and Potosnak et al. (2014) demonstrated that the ecosystem-scale response is dependent on
514 drought severity. Some studies have also reported an increase in isoprene after rewetting (e.g.
515 Brillì et al. 2007; Peñuelas et al., 2009; Sharkey & Loreto 1993). The isoprene measurements
516 made during the WIsDOM campaign (Ferracci et al., 2020 in prep) together with the findings
517 from our model simulations support the observation that isoprene emissions can increase
518 under moderate drought conditions and after rewetting resulting in strong enhancements in
519 canopy concentrations. Our model results (Figure S4) also provide evidence in support of the
520 previous observations that isoprene emissions and photosynthesis (often quantified as gross
521 primary production, GPP, at an ecosystem-scale; e.g Brillì et al., 2007; Pegoraro et al., 2004)
522 are uncoupled during periods of drought stress.

523 Emissions models have been shown to perform well in both the unstressed and severe
524 drought phases (e.g. Guenther et al., 2012; Emmerson et al., 2019; Jiang et al., 2019) but
525 underestimate observed concentrations during the mild-to-moderate drought phase (Potosnak
526 et al., 2014; Seco et al., 2015). Conceptual models (Niinemets, 2010; Potosnak et al., 2014)
527 have been developed to explain the impacts of mild droughts on isoprene emissions but these
528 have not been tested until now. We hypothesise that drought severity is the main determinant

529 of changes in isoprene emission rates at the ecosystem scale as well as in the laboratory and
530 that the previous field campaigns used to develop and verify the Guenther soil moisture
531 activity factor (see Pegoraro et al., 2004, Seco et al., 2015) encountered soil water deficits
532 that were more severe than those at Wytham Woods in 2018. Indeed, the Ozark site
533 (described in Gu et al., 2006) which has been used in parameterising the Guenther soil
534 moisture activity factor experienced two consecutive years of drought in 2011 (mild) and
535 2012 (severe). 2012 experienced the lowest rainfall in that decade and isoprene emissions
536 decreased significantly (Seco et al., 2015). However, similar to Wytham Woods, isoprene
537 fluxes were observed to increase at the Ozarks during the mild phase of the drought in 2011
538 (Potosnak et al., 2014).

539 Potosnak et al. (2014) hypothesized that an increase in leaf temperature due to
540 reductions in transpiration during drought stress is responsible for the increase in isoprene
541 emissions as emission rates depend on leaf rather than air temperature. We found that using a
542 leaf temperature-based isoprene emission activity factor did improve model reproduction of
543 observed isoprene mixing ratios but a substantial underestimation remained. We therefore
544 incorporated a soil moisture activity factor, based on the parameterisation of Keenan et al.
545 (2010) for changes in photosynthesis, that increases isoprene emissions under moderate
546 drought conditions, i.e. when SWC is close to but slightly above the critical value for the soil
547 at which the standard (severe drought) soil moisture activity factor can be applied. We found
548 that using this new activity factor to account for soil moisture stress when estimating isoprene
549 emission rates improved model reproduction of observed isoprene mixing ratios during the
550 moderate drought without compromising model performance during the rest of the season.
551 However, this was not in itself sufficient to capture the enhancement in isoprene
552 concentrations observed after rainfall events, when soil moisture increased substantially. We
553 found it necessary to further modify our activity factor to account for these episodes, on the
554 hypothesis that these rewetting events were of sufficient intensity to provide near-surface
555 roots access to water, leading to increased foliar activity and isoprene synthesis. Using this
556 soil water and rewetting-based modifying factor that increased isoprene emission rates a
557 further 30% improved the model fit to observations by 50% based on the root mean squared
558 error. In comparison, Brill et al., 2007 observed a 20-60% increase in isoprene emissions
559 from saplings following soil rewetting. These experimental modelling results provide
560 evidence that previous laboratory-based observations of the effect of mild-to-moderate
561 drought stress and soil rewetting on bVOC emissions (e.g. Brill et al., 2007; Centritto, Brill,

562 Fodale, & Loreto, 2011; Loreto & Schnitzler, 2010; Pegoraro et al, 2004a) are also
563 observable at the ecosystem-scale.

564 Many field sites do not routinely measure either soil moisture or leaf temperature;
565 our parameterisations are therefore only appropriate for model frameworks with a detailed
566 land surface module. We performed two further experiments using air temperature and
567 vapour pressure deficit (VPD), both readily available data products, as a proxy for the effects
568 of leaf temperature and soil water content. VPD, which can be readily calculated from
569 standard meteorological measurements, increases with increasing temperatures and declining
570 soil moisture. Although VPD is not a physiologically robust metric for assessing soil and
571 foliar water availability, we found that an isoprene emission activity factor based on VPD
572 improved modelled isoprene mixing ratios compared to the base case. Our air temperature
573 and VPD parameterisation and results are shown in Eqn S1 and S4, Figures S5-8 and Table
574 S1. Although not as successful as the rewetting simulations (for example there is a ~10% and
575 ~15% improvement on BASE RMSE in BASE+T and BASE+VPD respectively compared to
576 ~50% in BASE+RWT), our results show that VPD in particular could be used to improve
577 simulated emissions at sites where soil moisture or leaf temperature measurements are not
578 available and in models without a detailed land surface parameterisation.

579 The Guenther et al., 2006; 2012 algorithms reproduce observed isoprene concentrations
580 or fluxes well in unstressed environments and in cases of severe drought. The methods
581 developed in this paper are intended to be used in cases of mild-to-moderate drought which
582 until now has remained a modelling challenge.

583 Prior to the summer of 2018, Wytham Woods experienced only infrequent moderate to
584 severe droughts (in 1976, 1995-1997 and 2003; Mihók et al., 2009). It is projected that the
585 incidence of droughts in southern England will increase in frequency, duration and severity
586 under future climate change (e.g. Milly, Dunne, & Vecchia, 2005; Schär et al., 2004; Vidale,
587 Lüthi, Wegmann, & Schär, 2007). The summer of 2018 could therefore be viewed as a
588 'natural experiment' that allowed us to investigate possible future biogenic emissions from
589 Wytham Woods and similar temperate mixed woodlands. We found that the emissions
590 algorithms currently included in global emissions and chemistry-climate models
591 underestimated total isoprene emissions during the heatwave-drought by ~40% and by ~20%
592 over the entire June to September period. While the findings of this single experiment should
593 not be extrapolated to a global scale, if these are representative of the wider picture, the
594 magnitude of the modelled change in emissions would have a major impact on local- to

595 regional-scale emissions and hence atmospheric chemistry and composition in many world
596 regions.

597 The main advantage of our natural experiment is that we were able to observe the
598 impacts on mature trees in a real-world (uncontrolled) environment. Such conditions are
599 impossible to reproduce in laboratory-based experiments that investigate potential impacts of
600 global climate change on tree physiology and bVOC emissions. Saplings and young plants,
601 the preferred options in laboratory experiments, do provide useful information about the
602 general behaviour of trees under various environmental stressors, but cannot replicate the
603 combinatorial stresses and symbioses experienced by mature trees and full ecosystems. The
604 results from WISDOM and previous measurement campaigns carried out on mature trees (e.g.
605 Genard-Zielinski et al., 2018; Llusia et al., 2016; Potosnak et al., 2014) show that emissions
606 characteristics under heatwave-droughts in the natural environment differ from those
607 observed in many laboratory experiments. However, it can be expected for the response to be
608 dependent on tree species, with some adapted to withstand periods of water limitation, and on
609 soil properties. It is clear therefore that more ecosystem-scale observations are required under
610 mild, moderate and severe drought conditions if we are to understand how future changes in
611 precipitation and ground-water levels are to affect isoprene emissions.

612

613 **Acknowledgements**

614 F. Otu-Larbi is grateful to the Faculty of Science and Technology (FST) and Lancaster
615 Environment Centre (LEC) at Lancaster University for funding his PhD Studentship. K.
616 Ashworth is a Royal Society Dorothy Hodgkin Fellow and thanks the Royal Society of
617 London for their support and funding (DH150070). C. Bolas acknowledges and thanks the
618 Natural Environmental Research Council (NERC) for the Doctoral Training Partnership
619 studentship. The research was carried out and supported with funding from the BALI project
620 (NE/ K016377/1). In addition, we also thank the School of Geography and the Environment,
621 University of Oxford for help in instrument deployment and for supporting the walkway and
622 other research facilities at Wytham Woods research forest. In particular, we thank Nigel
623 Fisher for his day-to-day management of Wytham Woods research logistics and access. We
624 gratefully acknowledge R. Freshwater at the University of Cambridge for his technical
625 expertise and help. We are also grateful to the Environmental Change Network (ECN) for
626 sharing their data from the Upper Seeds automated weather station.

627

628 **Code and data availability:** FORCAsT 1.0 and the data used in this study are available by
629 request to the corresponding authors.

630

631 **References**

632

633 Arneth, A., Harrison, S. P., Zaehle, S., Tsigaridis, K., Menon, S., Bartlein, P. J., ... &
634 Schurgers, G. (2010). Terrestrial biogeochemical feedbacks in the climate system. *Nature*
635 *Geoscience*, 3(8), 525. <https://doi.org/10.1038/ngeo905>

636 Arneth, A., Monson, R. K., Schurgers, G., Niinemets, Ü., & Palmer, P. I. (2008). Why are
637 estimates of global terrestrial isoprene emissions so similar (and why is this not so for
638 monoterpenes)? *Atmospheric Chemistry and Physics*, 8(16), 4605-4620.
639 <https://doi.org/10.5194/acp-8-4605-2008>.

640 Ashworth, K., Chung, S. H., Griffin, R. J., Chen, J., Forkel, R., Bryan, A. M., & Steiner, A.
641 L. (2015). FORest Canopy Atmosphere Transfer (FORCAsT) 1.0: a 1-D model of biosphere–
642 atmosphere chemical exchange. *Geoscientific Model Development*, 8(11), 3765-3784.
643 <https://doi.org/10.5194/gmd-8-3765-2015>.

644 Baldwin, I. T. (2010). Plant volatiles. *Current Biology*, 20(9), R392-R397.
645 <https://doi.org/10.1016/j.cub.2010.02.052>.

646 Baldwin, I. T., Halitschke, R., Paschold, A., Von Dahl, C. C., & Preston, C. A. (2006).
647 Volatile signaling in plant-plant interactions: "talking trees" in the genomics era. *science*,
648 311(5762), 812-815. <https://doi.org/10.1126/science.1118446>.

649 Bamberger, I., Ruehr, N. K., Schmitt, M., Gast, A., Wohlfahrt, G., & Arneth, A. (2017).
650 Isoprene emission and photosynthesis during heatwaves and drought in black locust.
651 *Biogeosciences*, 14(15), 3649-3667. <https://doi.org/10.5194/bg-14-3649-2017>.

652 Bolas, C. G. (2020). *Forest Isoprene Emissions: New Insights from a Novel Field Instrument*
653 (Doctoral dissertation, University of Cambridge).

654 Bolas, C. G., Ferracci, V., Robinson, A. D., Mead, M. I., Nadzir, M. S. M., Pyle, J. A., Jones,
655 R. L., and Harris, N. R. P.: iDirac: a field-portable instrument for long-term autonomous
656 measurements of isoprene and selected VOCs, *Atmos. Meas. Tech. Discuss.*
657 <https://doi.org/10.5194/amt-2019-219>, in review, 2019

658 Brilli, F., Barta, C., Fortunati, A., Lerdau, M., Loreto, F., & Centritto, M. (2007). Response
659 of isoprene emission and carbon metabolism to drought in white poplar (*Populus alba*)
660 saplings. *New Phytologist*, 175(2), 244-254. [https://doi.org/10.1111/j.1469-](https://doi.org/10.1111/j.1469-8137.2007.02094.x)
661 8137.2007.02094.x.

662 Brüggemann, N., & Schnitzler, J. P. (2002). Comparison of isoprene emission, intercellular
663 isoprene concentration and photosynthetic performance in water-limited oak (*Quercus*
664 *pubescens* Willd. and *Quercus robur* L.) saplings. *Plant Biology*, 4(04), 456-463.
665 [https://doi.org/ 10.1055/s-2002-34128](https://doi.org/10.1055/s-2002-34128).

666 Bryan, A. M., Bertman, S. B., Carroll, M. A., Dusanter, S., Edwards, G. D., Forkel, R., ... &
667 Jobson, B. T. (2012). In-canopy gas-phase chemistry during CABINEX 2009: sensitivity of a
668 1-D canopy model to vertical mixing and isoprene chemistry. *Atmospheric Chemistry and*
669 *Physics*, 12(18), 8829-8849. <https://doi.org/10.5194/acp-12-8829-2012>.

670 Carlton, A. G., Wiedinmyer, C., & Kroll, J. H. (2009). A review of Secondary Organic
671 Aerosol (SOA) formation from isoprene. *Atmospheric Chemistry and Physics*, 9(14), 4987-
672 5005. [https://doi.org/ 10.5194/acp-9-4987-2009](https://doi.org/10.5194/acp-9-4987-2009).

673 Carslaw, K. S., Boucher, O., Spracklen, D. V., Mann, G. W., Rae, J. G. L., Woodward, S., &
674 Kulmala, M. (2010). A review of natural aerosol interactions and feedbacks within the Earth
675 system. *Atmospheric Chemistry and Physics*, 10(4), 1701-1737. [https://doi.org/ 10.5194/acp-](https://doi.org/10.5194/acp-10-1701-2010)
676 [10-1701-2010](https://doi.org/10.5194/acp-10-1701-2010).

677 Centritto, M., Brillì, F., Fodale, R., & Loreto, F. (2011). Different sensitivity of isoprene
678 emission, respiration and photosynthesis to high growth temperature coupled with drought
679 stress in black poplar (*Populus nigra*) saplings. *Tree physiology*, 31(3), 275-286.
680 <https://doi.org/10.1093/treephys/tpq1>.

681 Egea, G., Verhoef, A., & Vidale, P. L. (2011). Towards an improved and more flexible
682 representation of water stress in coupled photosynthesis–stomatal conductance models.
683 *Agricultural and Forest Meteorology*, 151(10), 1370-1384.
684 <https://doi.org/10.1016/j.agrformet.2011.05.019>.

685 Emmerson, K. M., Palmer, P. I., Thatcher, M., Haverd, V., & Guenther, A. B. (2019).
686 Sensitivity of isoprene emissions to drought over south-eastern Australia: Integrating models
687 and satellite observations of soil moisture. *Atmospheric Environment*, 209, 112-124.
688 <https://doi.org/10.1016/j.atmosenv.2019.04.038>.

689 Evans, R. C., Tingey, D. T., Gumpertz, M. L., & Burns, W. F. (1982). Estimates of isoprene
690 and monoterpene emission rates in plants. *Botanical Gazette*, 143(3), 304-310.
691 <https://doi.org/10.1086/botanicalgazette.143.3.2474826>.

692 Fuentes, J. D., Lerdau, M., Atkinson, R., Baldocchi, D., Bottenheim, J. W., Ciccioli, P., ... &
693 Sharkey, T. D. (2000). Biogenic hydrocarbons in the atmospheric boundary layer: a review.
694 *Bulletin of the American Meteorological Society*, 81(7), 1537-1576.
695 [https://doi.org/10.1175/1520-0477\(2000\)081<1537:BHITAB>2.3.CO;2](https://doi.org/10.1175/1520-0477(2000)081<1537:BHITAB>2.3.CO;2).

696 Genard-Zielinski, A.C., Boissard, C., Ormeno, E., Lathiere, J., Reiter, I.M., Wortham,
697 H., Orts, J.P., Temime-Roussel, B., Guenet, B., Bartsch, S., Gauquelin, T., Fernandez,
698 C., 2018. Seasonal variations of *Quercus pubescens* isoprene emissions from an in
699 natura forest under drought stress and sensitivity to future climate change in the Mediterranean
700 area. *Biogeosciences* 15, 4711–4730. <https://doi.org/10.5194/bg-15-4711-2018>.

701 Gu, L., Meyers, T., Pallardy, S. G., Hanson, P. J., Yang, B., Heuer, M., ... & Wullschlegel, S.
702 D. (2006). Direct and indirect effects of atmospheric conditions and soil moisture on surface
703 energy partitioning revealed by a prolonged drought at a temperate forest site. *Journal of*
704 *Geophysical Research: Atmospheres*, 111(D16). <https://doi.org/10.1029/2006JD007161>.

705 Guenther, A. B., Jiang, X., Heald, C. L., Sakulyanontvittaya, T., Duhl, T., Emmons, L. K., &
706 Wang, X. (2012). The Model of Emissions of Gases and Aerosols from Nature version 2.1
707 (MEGAN2. 1): an extended and updated framework for modeling biogenic emissions.
708 *Geoscientific Model Development*, 5(6), 1471-1492. [https://doi.org/10.5194/gmd-5-1471-](https://doi.org/10.5194/gmd-5-1471-2012)
709 2012. Guenther, A., Hewitt, C. N., Erickson, D., Fall, R., Geron, C., Graedel, T., ... & Pierce,
710 T. (1995). A global model of natural volatile organic compound emissions. *Journal of*
711 *Geophysical Research: Atmospheres*, 100(D5), 8873-8892.
712 <https://doi.org/10.1029/94JD02950>.

713 Guenther, A., Karl, T., Harley, P., Wiedinmyer, C., Palmer, P. I., & Geron, C. (2006).
714 Estimates of global terrestrial isoprene emissions using MEGAN (Model of Emissions of
715 Gases and Aerosols from Nature). *Atmospheric Chemistry and Physics*, 6(11), 3181-3210.
716 <https://doi.org/10.5194/acp-6-3181-2006>.

717 Heald, C. L., Wilkinson, M. J., Monson, R. K., Alo, C. A., Wang, G., & Guenther, A. (2009).
718 Response of isoprene emission to ambient CO₂ changes and implications for global budgets.
719 *Global Change Biology*, 15(5), 1127-1140. [https://doi.org/10.1111/j.1365-](https://doi.org/10.1111/j.1365-2486.2008.01802.x)
720 2486.2008.01802.x.

721 Heil, M., & Bueno, J. C. S. (2007). Within-plant signaling by volatiles leads to induction and
722 priming of an indirect plant defense in nature. *Proceedings of the National Academy of*
723 *Sciences*, 104(13), 5467-5472. <https://doi.org/10.1073/pnas.0610266104>

724 Herbst, M., Rosier, P. T., Morecroft, M. D., & Gowing, D. J. (2008). Comparative
725 measurements of transpiration and canopy conductance in two mixed deciduous woodlands
726 differing in structure and species composition. *Tree physiology*, 28(6), 959-970.
727 <https://doi.org/10.1093/treephys/28.6.959>.

728 Holopainen, J. K. (2004). Multiple functions of inducible plant volatiles. *Trends in plant*
729 *science*, 9(11), 529-533, doi.org/10.1016/j.tplants.2004.09.006.

730 IPCC (2001) *Climate Change 2001: The Scientific Basis*. Cambridge University Press,
731 Cambridge, UK.

732 IPCC [Intergovernmental Panel on Climate Change]. (2013). Near-term climate change:
733 Projections and predictability. *Stocker TF, Qin D, Plattner GK, Tignor M, Allen SK,*
734 *Boschung J, Nauels A, Xia Y, Bex V, Midgley PM, editors: Climate Change 2013: The*
735 *Physical Science Basis. Contribution of Working Group I to the Fifth Assessment Report of*
736 *the Intergovernmental Panel on Climate Change*, 978-980.

737 Jiang, X., Guenther, A., Potosnak, M., Geron, C., Seco, R., Karl, T., ... & Pallardy, S. (2018).
738 Isoprene emission response to drought and the impact on global atmospheric chemistry.
739 *Atmospheric Environment*, 183, 69-83. <https://doi.org/10.1016/j.atmosenv.2018.01.026>.

740 Keenan, T., Sabate, S., & Gracia, C. (2010). Soil water stress and coupled photosynthesis–
741 conductance models: Bridging the gap between conflicting reports on the relative roles of
742 stomatal, mesophyll conductance and biochemical limitations to photosynthesis. *Agricultural*
743 *and Forest Meteorology*, 150(3), 443-453. <https://doi.org/10.1016/j.agrformet.2010.01.008>.

744 Kirby, K. J., Bazely, D. R., Goldberg, E. A., Hall, J. E., Isted, R., Perry, S. C., & Thomas, R.
745 C. (2014). Changes in the tree and shrub layer of Wytham Woods (Southern England) 1974–
746 2012: local and national trends compared. *Forestry: An International Journal of Forest*
747 *Research*, 87(5), 663-673. <https://doi.org/10.1093/forestry/cpu026>.

748 Laothawornkitkul, J., Taylor, J. E., Paul, N. D., & Hewitt, C. N. (2009). Biogenic volatile
749 organic compounds in the Earth system. *New Phytologist*, 183(1), 27-51.
750 <https://doi.org/10.1111/j.1469-8137.2009.02859.x>.

751 Lerdau, M., & Keller, M. (1997). Controls on isoprene emission from trees in a subtropical
752 dry forest. *Plant, Cell & Environment*, 20(5), 569-578. <https://doi.org/10.1111/j.1365-3040.1997.00075.x>.

754 Llusia, J., Roahtyn, S., Yakir, D., Rotenberg, E., Seco, R., Guenther, A., & Penuelas, J.
755 (2016). Photosynthesis, stomatal conductance and terpene emission response to water
756 availability in dry and mesic Mediterranean forests. *Trees*, 30(3), 749-759.
757 <https://doi.org/10.1007/s00468-015-1317-x>.

758 Loreto, F., & Schnitzler, J. P. (2010). Abiotic stresses and induced BVOCs. *Trends in plant*
759 *science*, 15(3), 154-166. <https://doi.org/10.1016/j.tplants.2009.12.006>.

760 Loreto, F., & Velikova, V. (2001). Isoprene produced by leaves protects the photosynthetic
761 apparatus against ozone damage, quenches ozone products, and reduces lipid peroxidation of
762 cellular membranes. *Plant Physiology*, 127(4), 1781-1787.
763 <https://doi.org/10.1104/pp.010497>.

764 Lüpke, M., Leuchner, M., Steinbrecher, R., & Menzel, A. (2017). Impact of summer drought
765 on isoprenoid emissions and carbon sink of three Scots pine provenances. *Tree physiology*, 1-
766 1. <https://doi.org/10.1093/treephys/tpw066>.

767 Makar, P. A., Staebler, R. M., Akingunola, A., Zhang, J., McLinden, C., Kharol, S. K., ... &
768 Zheng, Q. (2017). The effects of forest canopy shading and turbulence on boundary layer
769 ozone. *Nature communications*, 8, 15243. <https://doi.org/10.1038/ncomms15243>.

770 McKee, T. B., Doesken, N. J., & Kleist, J. (1993). The relationship of drought frequency and
771 duration to time scales. In *Proceedings of the 8th Conference on Applied Climatology* (Vol.
772 17, No. 22, pp. 179-183). Boston, MA: American Meteorological Society.

773 Mihók, B., Kenderes, K., Kirby, K. J., Paviour-Smith, K., & Elbourn, C. A. (2009). Forty-
774 year changes in the canopy and the understorey in Wytham Woods. *Forestry*, 82(5), 515-527.
775 <https://doi.org/10.1093/forestry/cpp021>.

776 Milly, P. C., Dunne, K. A., & Vecchia, A. V. (2005). Global pattern of trends in streamflow
777 and water availability in a changing climate. *Nature*, 438(7066), 347.
778 <https://doi.org/10.1038/nature04312>.

779 Monthly, seasonal and annual summaries 2018 (2019), Retrieved October 16, 2019, from UK
780 Met Office website: [https://www.metoffice.gov.uk/research/climate/maps-and-](https://www.metoffice.gov.uk/research/climate/maps-and-data/summaries/index)
781 [data/summaries/index](https://www.metoffice.gov.uk/research/climate/maps-and-data/summaries/index)

782 Morecroft, M. D., Stokes, V. J., Taylor, M. E., & Morison, J. I. (2008). Effects of climate and
783 management history on the distribution and growth of sycamore (*Acer pseudoplatanus* L.) in
784 a southern British woodland in comparison to native competitors. *Forestry*, 81(1), 59-74,
785 <https://doi.org/10.1093/forestry/cpm045>.

786 Morfopoulos, C., Prentice, I. C., Keenan, T. F., Friedlingstein, P., Medlyn, B. E., Peñuelas, J.,
787 & Possell, M. (2013). A unifying conceptual model for the environmental responses of
788 isoprene emissions from plants. *Annals of botany*, 112(7), 1223-1238.
789 <https://doi.org/10.1093/aob/mct206>.

790 Niinemets, Ü. (2010). Mild versus severe stress and BVOCs: thresholds, priming and
791 consequences. *Trends in plant science*, 15(3), 145-153.
792 <https://doi.org/10.1016/j.tplants.2009.11.008>.

793 Pacifico, F., Harrison, S. P., Jones, C. D., & Sitch, S. (2009). Isoprene emissions and climate.
794 *Atmospheric Environment*, 43(39), 6121-6135.
795 <https://doi.org/10.1016/j.atmosenv.2009.09.002>.

796 Pegoraro, E., Abrell, L., Van Haren, J., Barron-Gafford, G., Grieve, K. A., Malhi, Y., ... &
797 Lin, G. (2005). The effect of elevated atmospheric CO₂ and drought on sources and sinks of

798 isoprene in a temperate and tropical rainforest mesocosm. *Global Change Biology*, 11(8),
799 1234-1246. <https://doi.org/10.1111/j.1365-2486.2005.00986.x>.

800 Pegoraro, E., Rey, A., Greenberg, J., Harley, P., Grace, J., Malhi, Y., & Guenther, A. (2004).
801 Effect of drought on isoprene emission rates from leaves of *Quercus virginiana* Mill.
802 *Atmospheric Environment*, 38(36), 6149-6156.
803 <https://doi.org/10.1016/j.atmosenv.2004.07.028>.

804 Peñuelas, J., & Llusà, J. (2002). Linking photorespiration, monoterpenes and
805 thermotolerance in *Quercus*. *New Phytologist*, 155(2), 227-237.
806 <https://doi.org/10.1046/j.1469-8137.2002.00457.x>.

807 Peñuelas, J., Filella, I., Seco, R., & Llusia, J. (2009). Increase in isoprene and monoterpene
808 emissions after re-watering of droughted *Quercus ilex* seedlings. *Biologia plantarum*, 53(2),
809 351-354. <https://doi.org/10.1007/s10535-009-0065-4>.

810 Pike, R. C., & Young, P. J. (2009). How plants can influence tropospheric chemistry: the role
811 of isoprene emissions from the biosphere. *Weather*, 64(12), 332-336. [https://doi.org/](https://doi.org/10.1002/wea.416)
812 [10.1002/wea.416](https://doi.org/10.1002/wea.416).

813 Pollastri, S., Tsonev, T., & Loreto, F. (2014). Isoprene improves photochemical efficiency
814 and enhances heat dissipation in plants at physiological temperatures. *Journal of*
815 *experimental botany*, 65(6), 1565-1570. <https://doi.org/10.1093/jxb/eru033>.

816 Potosnak, M. J., LeSturgeon, L., Pallardy, S. G., Hosman, K. P., Gu, L., Karl, T., ... &
817 Guenther, A. B. (2014). Observed and modeled ecosystem isoprene fluxes from an oak-
818 dominated temperate forest and the influence of drought stress. *Atmospheric environment*, 84,
819 314-322. <https://doi.org/10.1016/j.atmosenv.2013.11.055>.

820 Regional Values. (2019). Retrieved June 1, 2019, from UK Met Office website:
821 <https://www.metoffice.gov.uk/climate/uk/summaries/2018/summer/regional-values>
822 Rennenberg, H., Loreto, F., Polle, A., Brilli, F., Fares, S., Beniwal, R. S., & Gessler, A.
823 (2006). Physiological responses of forest trees to heat and drought. *Plant Biology*, 8(05), 556-
824 571. <https://doi.org/10.1055/s-2006-924084>.
825 Sanderson, M. G., Jones, C. D., Collins, W. J., Johnson, C. E., & Derwent, R. G. (2003).
826 Effect of climate change on isoprene emissions and surface ozone levels. *Geophysical*
827 *Research Letters*, 30(18). <https://doi.org/10.1029/2003GL017642>.
828 Schär C, Vidale P. L, Lüthi D, Frei C, Häberli C, Liniger MA, Appenzeller C (2004) The role
829 of increasing temperature variability for European summer heat waves. *Nature* 427:332–336.
830 <https://doi.org/10.1038/nature02300>
831 Seco, R., Karl, T., Guenther, A., Hosman, K. P., Pallardy, S. G., Gu, L., ... & Kim, S. (2015).
832 Ecosystem-scale volatile organic compound fluxes during an extreme drought in a broadleaf
833 temperate forest of the Missouri Ozarks (central USA). *Global change biology*, 21(10), 3657-
834 3674. <https://doi.org/10.1111/gcb.12980>.
835 Sharkey, T. D. (1996). Isoprene synthesis by plants and animals. *Endeavour*, 20(2), 74-78.
836 [https://doi.org/10.1016/0160-9327\(96\)10014-4](https://doi.org/10.1016/0160-9327(96)10014-4).
837 Sharkey, T. D. (2000). Biogenic hydrocarbons in the atmospheric boundary layer: a review.
838 *Bulletin of the American Meteorological Society*, 81(7), 1537-1576.
839 [https://doi.org/10.1175/1520-0477\(2000\)081<1537:BHITAB>2.3.CO;2](https://doi.org/10.1175/1520-0477(2000)081<1537:BHITAB>2.3.CO;2).
840 Sharkey, T.D., Loreto, F. (1993). Water-stress, temperature, and light effects on the capacity
841 for isoprene emission and photosynthesis of kudzu leaves. *Oecologia* 95 (3), 328–333.
842 <https://doi.org/10.1007/BF00320984>.
843 Shuttleworth, W. J., & Wallace, J. S. (1985). Evaporation from sparse crops-an energy
844 combination theory. *Quarterly Journal of the Royal Meteorological Society*, 111(469), 839-
845 855. <https://doi.org/10.1002/qj.49711146910>.
846 Sindelarova, K., Granier, C., Bouarar, I., Guenther, A., Tilmes, S., Stavrakou, T., ... & Knorr,
847 W. (2014). Global data set of biogenic VOC emissions calculated by the MEGAN model
848 over the last 30 years. *Atmospheric Chemistry and Physics*, 14(17), 9317-9341.
849 <https://doi.org/10.5194/acp-14-9317-2014>.
850 Stocker, T. F.; Qin, D.; Plattner, G.-K.; Tignor, M. M. B.; Allen, S. K.; Boschung, J.; Nauels,
851 A.; Xia, Y.; Bex, V.; Midgley, P. M. (eds.) (2014). *Climate Change 2013: The Physical*
852 *Science Basis. Contribution of Working Group I to the Fifth Assessment Report of IPCC the*

853 *Intergovernmental Panel on Climate Change. Cambridge: Cambridge University Press.*
854 <https://doi.org/10.1017/CBO9781107415324>

855 Stroud, C., Makar, P., Karl, T., Guenther, A., Geron, C., Turnipseed, A., ... & Fuentes, J. D.
856 (2005). Role of canopy-scale photochemistry in modifying biogenic-atmosphere exchange of
857 reactive terpene species: Results from the CELTIC field study. *Journal of Geophysical*
858 *Research: Atmospheres*, 110(D17). <https://doi.org/10.1029/2005JD005775>.

859 Taylor, K. E. (2001). Summarizing multiple aspects of model performance in a single
860 diagram. *Journal of Geophysical Research: Atmospheres*, 106(D7), 7183-7192.
861 <https://doi.org/10.1029/2000JD900719>.

862 Thomas, M. V., Malhi, Y., Fenn, K. M., Fisher, J. B., Morecroft, M. D., Lloyd, C. R., ... &
863 McNeil, D. D. (2010). Carbon dioxide fluxes over an ancient broadleaved deciduous
864 woodland in southern England. *Biogeosciences Discussions*, 7(3). [https://doi.org/10.5194/bg-](https://doi.org/10.5194/bg-8-1595-2011)
865 [8-1595-2011](https://doi.org/10.5194/bg-8-1595-2011).

866 Thornton, P. K., Ericksen, P. J., Herrero, M., & Challinor, A. J. (2014). Climate variability
867 and vulnerability to climate change: a review. *Global change biology*, 20(11), 3313-3328.
868 <https://doi.org/10.1111/gcb.12581>.

869 Tingey, D. T., Evans, R., & Gumpertz, M. (1981). Effects of environmental conditions on
870 isoprene emission from live oak. *Planta*, 152(6), 565-570.
871 <https://doi.org/10.1007/BF00380829>.

872 UK Extreme Events – Heatwaves. (2019). Retrieved June 1, 2019, from UK Met Office
873 website: [https://www.metoffice.gov.uk/research/climate/understanding-climate/uk-extreme-](https://www.metoffice.gov.uk/research/climate/understanding-climate/uk-extreme-events_heatwaves)
874 [events_heatwaves](https://www.metoffice.gov.uk/research/climate/understanding-climate/uk-extreme-events_heatwaves)

875 Unger, N. (2014). On the role of plant volatiles in anthropogenic global climate change.
876 *Geophysical Research Letters*, 41(23), 8563-8569. <https://doi.org/10.1002/2014GL061616>.

877 V. Ferracci, C.G. Bolas, R.A. Freshwater, Z. Staniaszek, K. Jaars, F. Otu-Larbi, T. King, J.
878 Beale, Y. Malhi, T.W. Waine, R.L. Jones, K. Ashworth, N.R.P. Harris, Continuous isoprene
879 measurements in a UK temperate forest for a whole growing season: effects of drought stress
880 during the 2018 heatwave, in preparation Ferracci 2020.

881 Vickers CE, Gershenzon J, Lerdau MT, Loreto F (2009). A unified mechanism of action for
882 isoprenoids in plant abiotic stress. *Nat Chem Biol* (5),283-291.
883 <https://doi.org/10.1038/nchembio.158>.

884 Vidale, P. L., Lüthi, D., Wegmann, R., & Schär, C. (2007). European summer climate
885 variability in a heterogeneous multi-model ensemble. *Climatic Change*, *81*(1), 209-232.
886 <https://doi.org/10.1007/s10584-006-9218-z>.

887 Visakorpi, K., Gripenberg, S., Malhi, Y., Bolas, C., Oliveras, I., Harris, N., ... & Riutta, T.
888 (2018). Small-scale indirect plant responses to insect herbivory could have major impacts on
889 canopy photosynthesis and isoprene emission. *New Phytologist*, *220*(3), 799-810.
890 <https://doi.org/10.1111/nph.15338>.

891 Zandalinas, S. I., Mittler, R., Balfagón, D., Arbona, V., & Gómez-Cadenas, A. (2018). Plant
892 adaptations to the combination of drought and high temperatures. *Physiologia plantarum*,
893 *162*(1), 2-12, <https://doi.org/10.1111/ppl.12540>.

894 Zimmer, W., Brüggemann, N., Emeis, S., Giersch, C., Lehning, A., Steinbrecher, R., &
895 Schnitzler, J. P. (2000). Process-based modelling of isoprene emission by oak leaves. *Plant*,
896 *Cell & Environment*, *23*(6), 585-595. <https://doi.org/10.1046/j.1365-3040.2000.00578.x>.

897

898 **FIGURE CAPTIONS**

899 Figure 1: Meteorological data taken from the Wytham Woods Automatic ECN station: (a)
900 Photosynthetically Active Radiation (PAR) (b) 2-m air temperature, (c) soil water content
901 (SWC; black) and total daily rainfall (blue). The grey shaded area indicates the start and end
902 of the heatwave-drought while the white dashed line indicates the start of the rewetting period
903 (20th July – 8th August).

904

905 Figure 2: Observed (black) and modelled (BASE; orange) isoprene mixing ratios at the
906 WISDOM site at (a) the top of the canopy (~15.6 m), (b) mid canopy (~13.5 m), (c) trunk
907 height (~7.1 m) and (d) near the surface (~0.8 m). Observations of isoprene mixing ratios at
908 the trunk and near surface levels started on 6th July.

909

910 Figure 3: (a) Difference (in ppb) between model (BASE) and observed (OBS) isoprene
911 mixing ratio at the top of the canopy for the BASE simulation for the entire season (1st June
912 to 30th September 2018). Note that negative values indicate periods when the model
913 underestimates concentrations while positive values indicate an overestimation. (b) Diurnal
914 profiles of isoprene mixing ratios at the top of the canopy before heatwave-drought (black),
915 during the heatwave drought (orange) and after the heatwave-drought (red). Model values are
916 solid lines while observed values are dashed lines. Scatter plots of difference in mixing ratio

917 vs. (c) soil water content (SWC) coloured by temperature and (d) leaf temperature coloured
918 by SWC.

919

920 Figure 4: Observed (OBS) and modelled (MOD) isoprene mixing ratios at the top (15.6 m; a-
921 c) and middle (13.5 m; d-f) of the canopy. Observations are shown in black and model
922 results in red (BASE+LFT), green (BASE+SWT), and blue (BASE+RWT). Figure S2 in the
923 SI shows similar results for the trunk and near-surface levels.

924

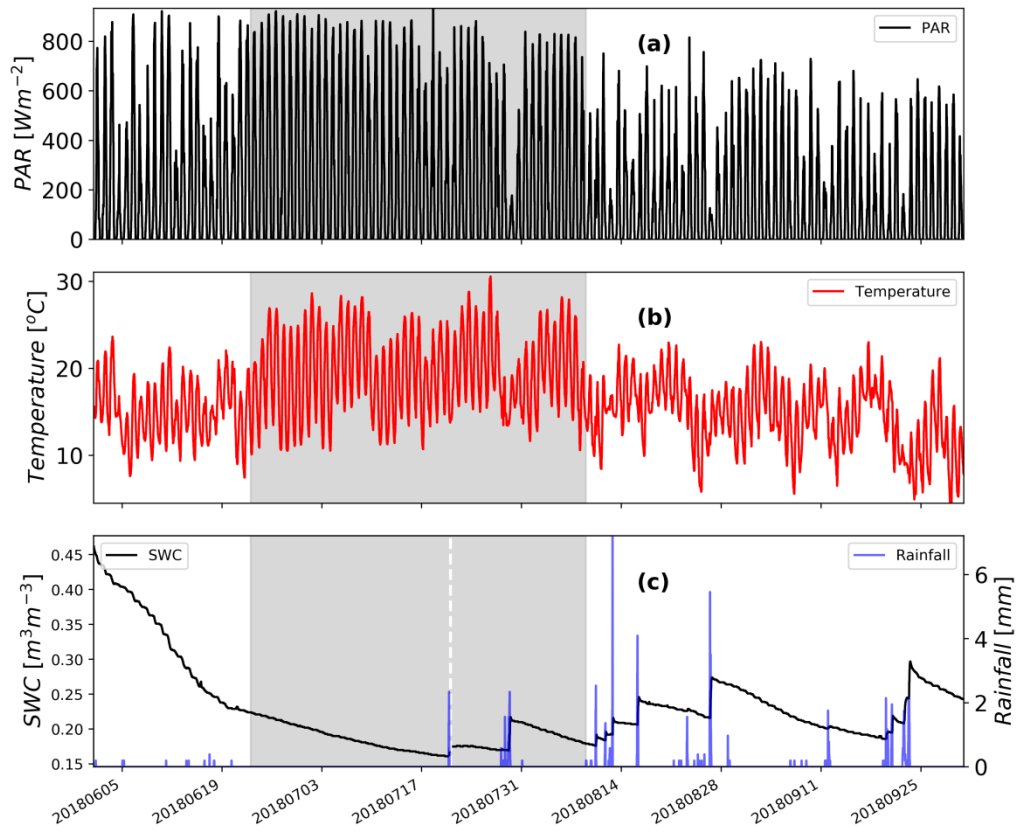
925 Figure 5: Scatter plots of model (MOD) and observed (OBS) isoprene (C_5H_8) mixing ratios
926 for (a and e) BASE coloured by SWC, (b and f) BASE+LFT coloured by SWC, (c and g)
927 BASE+SWT coloured by temperature, (d and h) BASE+RWT coloured by temperature.
928 Panels (a-d) show the top of the canopy (15.6 m) and panels (e-h) the middle of the canopy
929 (13.5 m). Figure S3 in the SI reproduces these scatter plots for the trunk and near surface
930 levels.

931

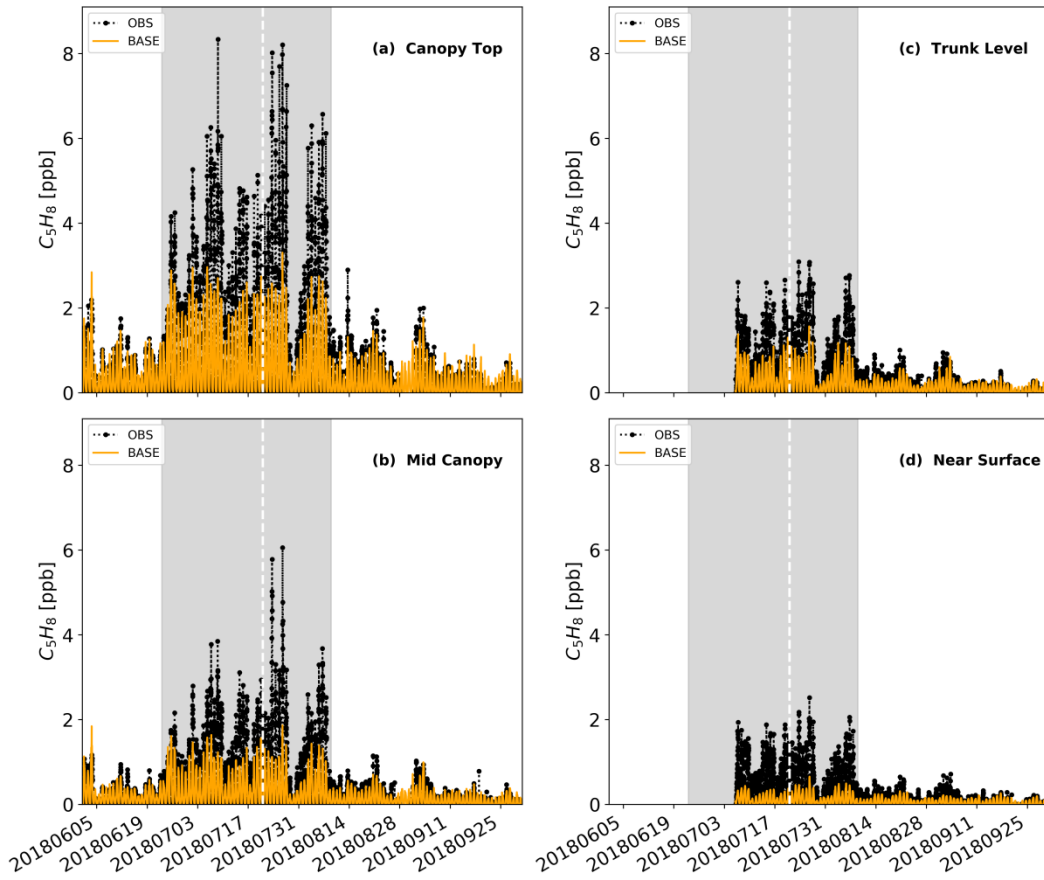
932 Figure 6: Taylor Diagram showing model output statistics from the four simulations for (a)
933 top of canopy (15.6m), (b) middle of canopy (13.5m), (c) trunk level (7.1m) and (d) near
934 surface (0.8m). Dashed black and brown curves and solid blue lines show normalised
935 standard deviation, centred root mean squared error (RMS error) and correlation coefficients
936 respectively against observations. The observed isoprene mixing ratios are summarised by the
937 purple circle with a normalised standard deviation of 1.0, RMS error of 0.0 and correlation of
938 1.0. The summary statistics for the four model simulations are shown by orange (BASE), red
939 (BASE+LFT), green (BASE+SWT), and blue (BASE+RWT) circles. Note the change in
940 scale of standard deviation on panel (c).

941

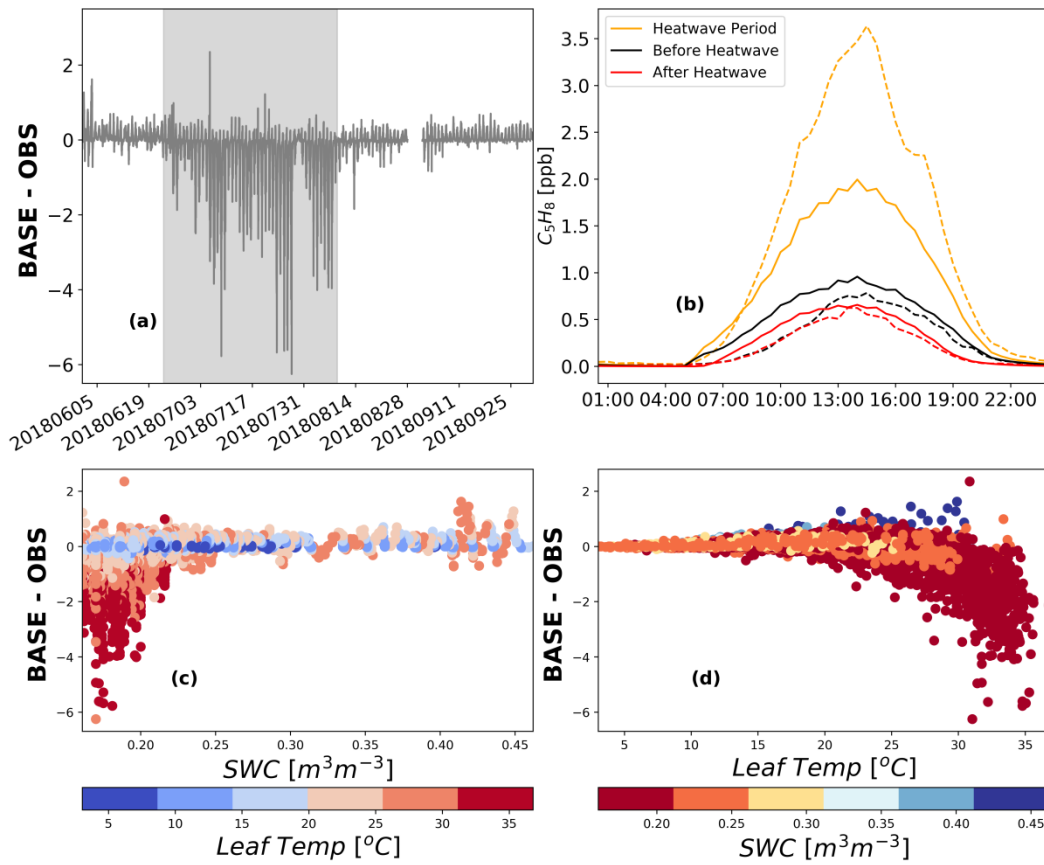
942 Figure 7 (a-d) Time series of isoprene mixing ratios for a selected period during the
943 heatwave-drought (22nd-27th July 2018) and (e-h) average diurnal profiles of isoprene mixing
944 ratios for the same period. Black dashed lines are observations while the models are coloured
945 orange (BASE), red (BASE+LFT), green (BASE+SWT) and blue (BASE+RWT). The grey
946 shading indicates the uncertainty limits ($\pm 11\%$) around the observations. (a) and (e), (b) and
947 (f), (c) and (g) and (d) and (h) are top of canopy, middle of canopy, trunk and near-surface
948 levels respectively.



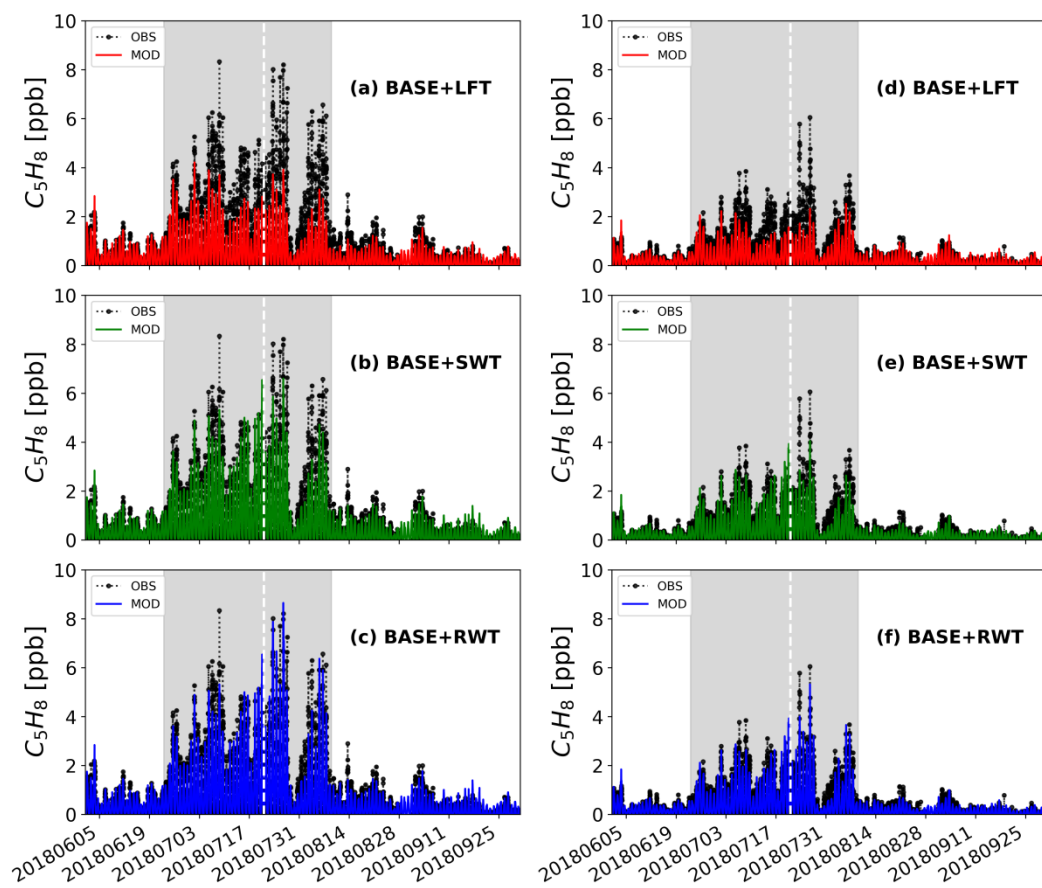
gcb_14963_f1.png



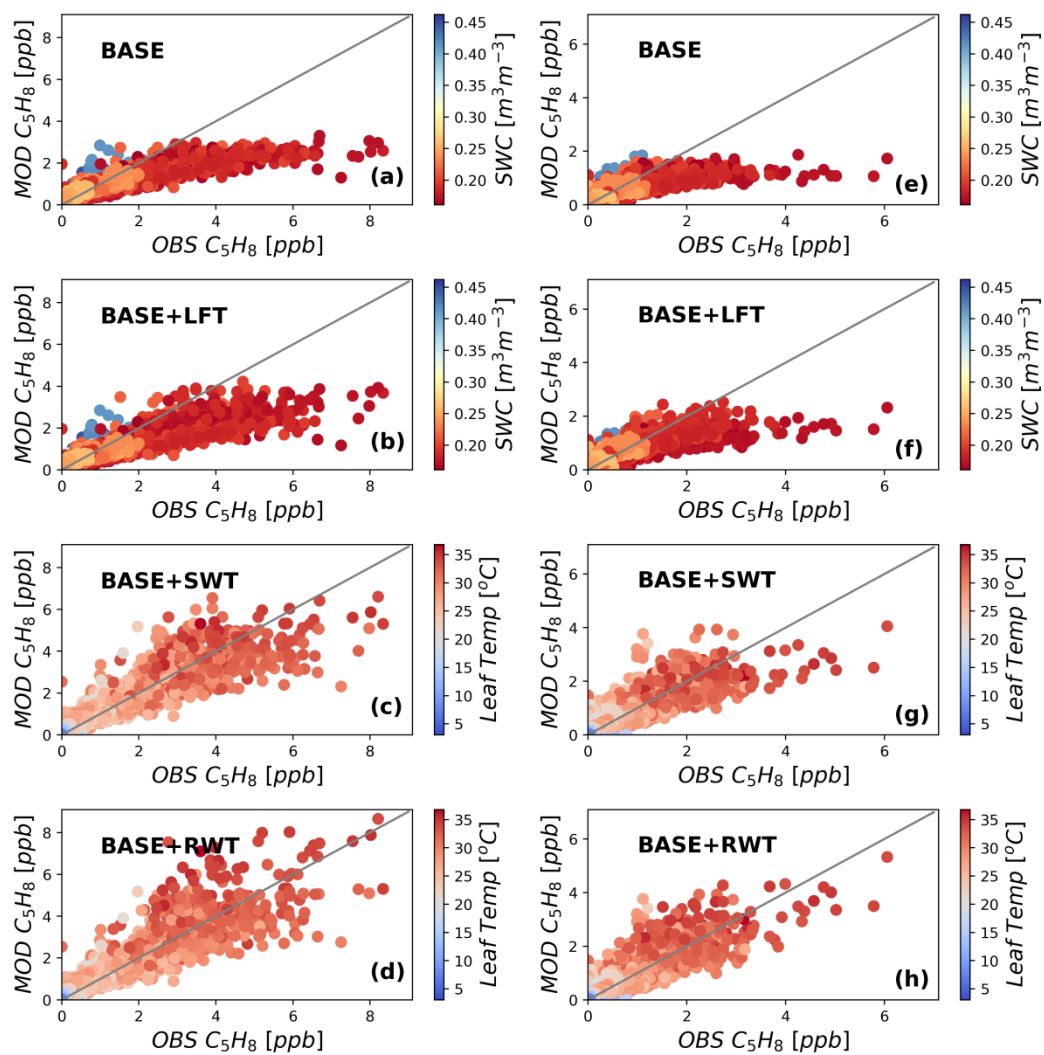
gcb_14963_f2.png



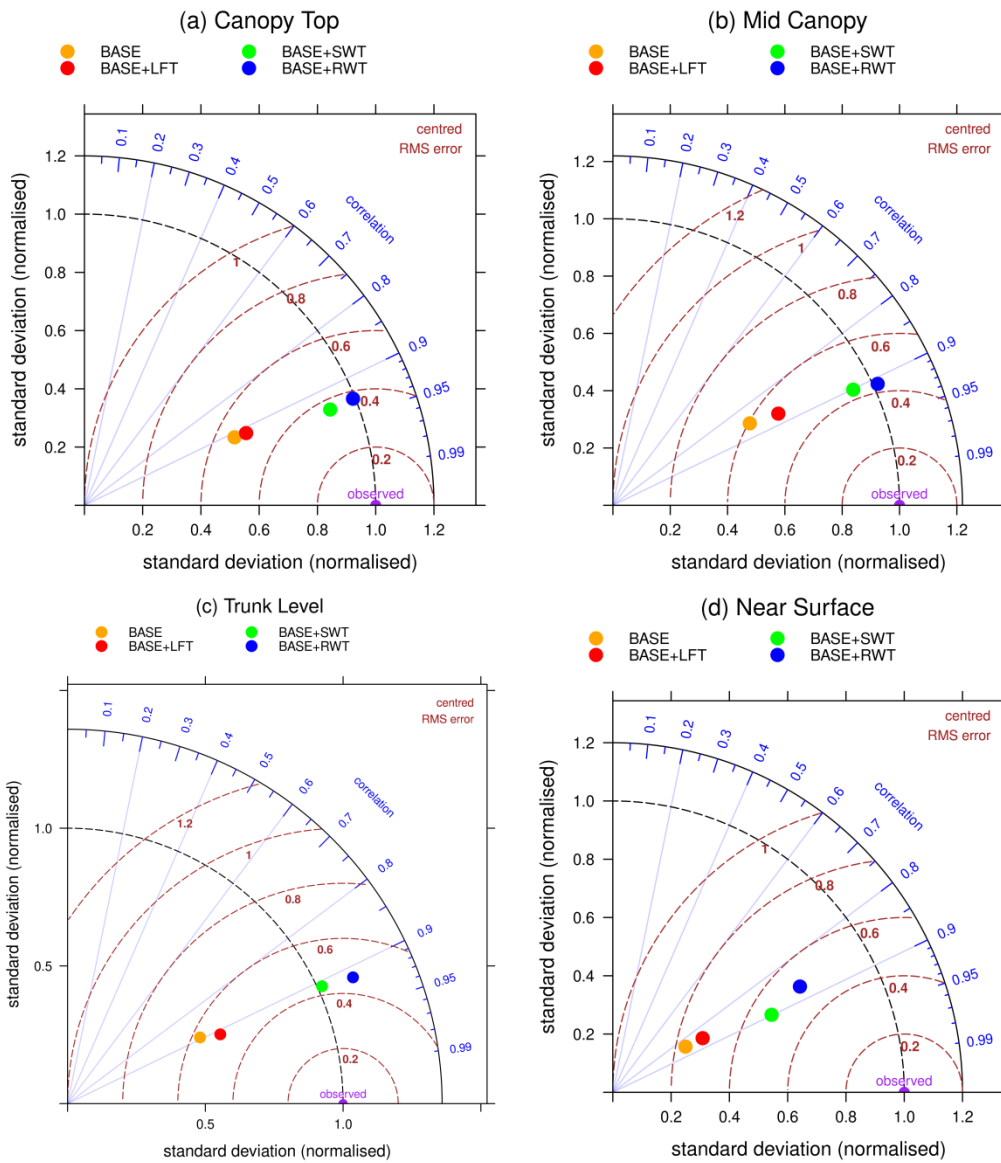
gcb_14963_f3.png



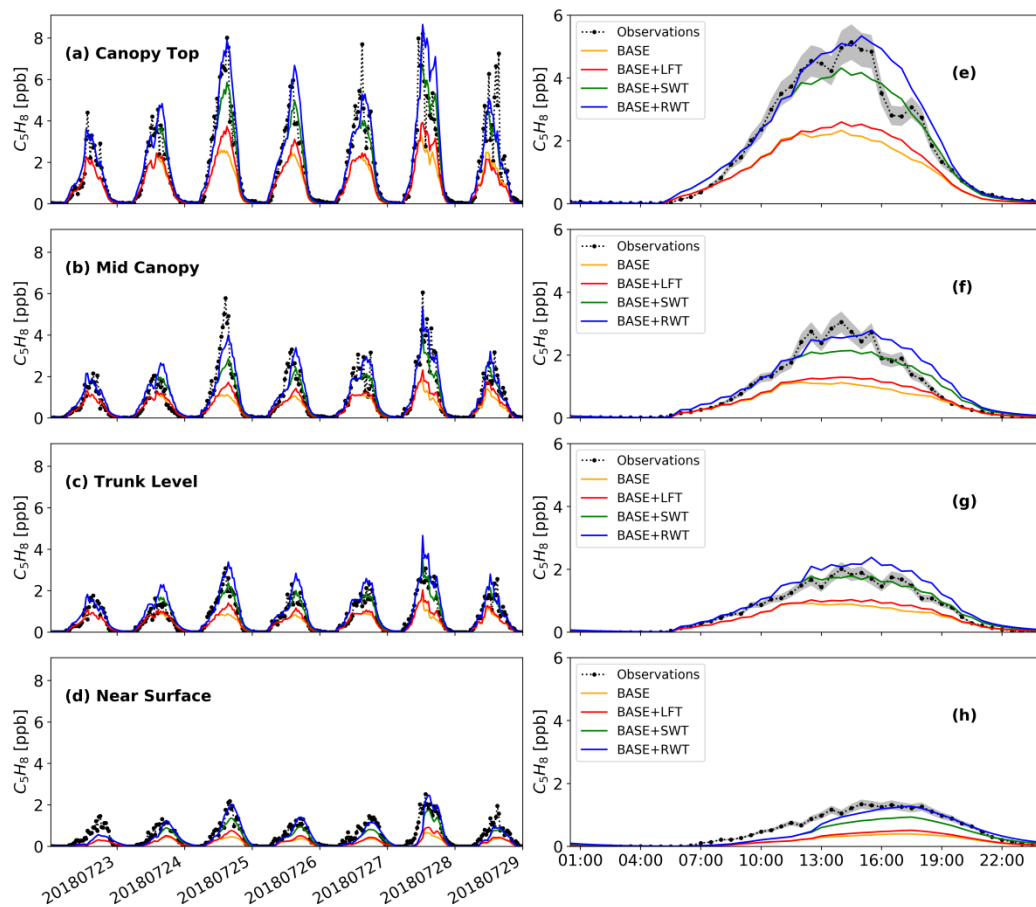
gcb_14963_f4.png



gcb_14963_f5.png



gcb_14963_f6.png



gcb_14963_f7.png